

Direct Observation of the Modulation of the 4*f*-Electron Orbital State by Strong *p*-*f* Mixing in CeSb

Kazuaki Iwasa,¹ Abdul Hannan,¹ Masahumi Kohgi,¹ and Takashi Suzuki²

¹*Department of Physics, Faculty of Science, Tokyo Metropolitan University, Hachioji, Tokyo 192-0397, Japan*

²*Tsukuba Institute of Science and Technology, Tsukuba, Ibaraki 300-0819, Japan*

(Received 10 October 2001; published 30 April 2002)

Low-temperature x-ray diffraction experiment has been carried out to investigate the 4*f*-electron state of the low carrier density system CeSb which shows complicated magnetic phase diagrams at low temperatures. The scattering pattern of the satellite peaks observed in the magnetically ordered state AFP3 is explained well by the model which takes into account both the lattice and charge modulations corresponding to the complex magnetic structure. The present result gives direct evidence for the strong modulation of the 4*f*-electron orbital state in CeSb due to the combined effect of the strong *p*-*f* mixing and carrier localization.

DOI: 10.1103/PhysRevLett.88.207201

PACS numbers: 75.10.Dg, 61.10.Eq, 61.50.Ks, 71.27.+a

Electron orbital degree of freedom has been understood to play an important role in physical properties of strongly correlated electron systems. For example, the phase transitions in CeB₆ [1] and TmTe [2] are explained by the ordering of the 4*f*-electron orbital states. In principle, the orbital ordering can be investigated microscopically by diffraction techniques. However, the anisotropy of the valence-electron orbits in heavy atoms is difficult to be observed by x-ray diffraction, because the core electrons contribute dominantly to scattering amplitudes. Recently, resonant scattering of synchrotron radiation x-ray succeeded in the observation of orbital ordering in LaMnO₃ [3], DyB₂C₂ [4], and so on. However, direct observation of orbital state to determine wave function of the 4*f* electrons has not been achieved yet.

The 4*f*-electron states of cerium monpnictides CeX (X = P, As, Sb, and Bi), which crystallize in a simple rocksalt structure, have been studied extensively, because of their unusual physical properties such as complicated magnetic phase diagrams under magnetic fields or under high pressures and resistivity anomaly like in dense Kondo systems [5]. One of them, CeSb, shows various long-period magnetic structures below $T_N = 17$ K even at ambient condition [6], as quoted in Fig. 1. The magnetic structures in the so-called antiferropara- (AFP) phases are composed of ferromagnetic and paramagnetic Ce (0 0 1) layers which stack with various sequences. Arrows and circles in the figure correspond to these layers, respectively. The magnitudes of magnetic moments of Ce ions in the ferromagnetic layers is $2\mu_B$ per Ce ion, and their direction is along the [0 0 1] axis. The crystal-field ground state of Ce³⁺ ions of CeSb in the paramagnetic phase is the Γ_7 doublet whose magnetic moment is $0.71\mu_B$. On the other hand, the excited state Γ_8 with a larger magnetic moment of $1.57\mu_B$ is located at an energy of about 37 K [7], which is anomalously lower than those of other rare-earth monpnictides. It is noted that the large value of $2\mu_B$ in the ordered phases is closer to that of the Γ_8 state. Takahashi and Kasuya ascribed the unusual mag-

netic properties of CeSb and CeBi to the strong magnetic polaron effect produced by the combination of localization of the low-density carriers and the mixing effect between the Γ_8 state of Ce ions and the *p* state of the neighboring pnictogens (*p*-*f* mixing) within the ferromagnetic layers [8]. Cooper and co-workers also presented a theory based on a Coqblin-Schrieffer model dealing with a hybridization effect involving *f*-electron states [9]. In addition, magnetic excitation and critical behavior on the magnetic ordering process of CeAs and CeSb investigated by neutron scattering experiments were explained phenomenologically by a quadrupolar interaction between Ce ions arising from the Γ_8 character [10].

Recent neutron-scattering studies of CeP and CeAs revealed that they show also long period magnetic structures in which ferromagnetically coupled Ce-ion double layers with the magnetic moment of about $2\mu_B$ appear periodically among the Γ_7 Ce-ion layers with the smaller magnetic moments under magnetic fields or under high

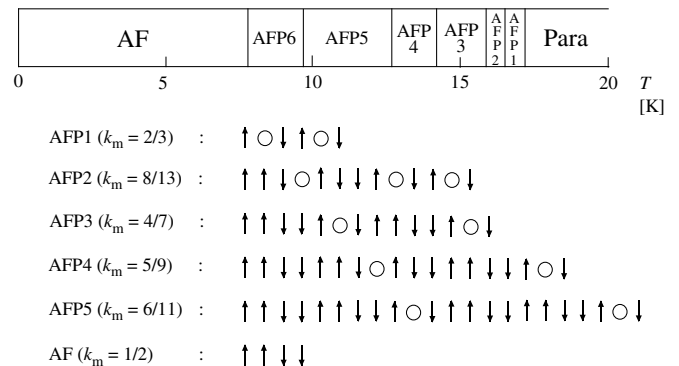


FIG. 1. Magnetic phase diagram of CeSb at ambient condition and schematic representations of magnetic structures [6]. Arrows indicate ordered Ce-ion layers with magnetic moments of $2\mu_B/\text{Ce}$, and circles indicate paramagnetic ones. Fundamental wave numbers of the magnetic structures, k_m , are in units of $2\pi/c$, where c corresponds to a lattice constant of the rocksalt structure.

pressures [11,12]. Some of their magnetic structures at higher pressures are similar to those of CeSb. Therefore, the Ce ions with the large ordered moments can be regarded as in a Γ_8 -like state and those in the paramagnetic layers as in the Γ_7 state.

The ordering of the two $4f$ -electron states in CeX also causes crystal-lattice modulation. The crystal structure of CeSb and CeBi transforms from a cubic structure to a tetragonal one accompanied by a sudden contraction of their crystal lattices, when the Ce ions with $2\mu_B$ appear below T_N [13,14]. Furthermore, temperature dependences of lattice constants of CeX show local minimum above T_N [13–15]. In the previous paper of x-ray study on CeSb, we reported satellite peaks in the AFP phases indicating long-period crystal-lattice modulations [16]. The observed scattering patterns were explained by the lattice modulation due to the periodically arranged different interlayer spacings caused by the difference of the effective ionic size between Γ_8 -like and Γ_7 Ce-ion layers. The crystal-lattice-modulation model also explains well the tetragonal distortion described above. In the present study, we found, moreover, that the complete interpretation of the x-ray data in the wide reciprocal space was not achieved only by the lattice modulation model. The experimental result clearly demonstrates that charge density modulation due to the existence of two different orbital states of Ce ions is also responsible for the scattering patterns. A brief report on the experimental results and discussion is given below.

We measured x-ray diffraction intensities along the reciprocal-lattice line $[0, 0, \xi]$ with $1 < \xi < 10$ of CeSb in the AFP3 phase. A cleaved single-crystal sample with a clean flat surface of the $(0\ 0\ 1)$ plane was mounted in a closed-cycle refrigerator, and it was installed on an x-ray spectrometer equipped with a rotating anode of Mo. A monochromator and an analyzer of pyrolytic graphite crystals were adopted to select only the K_{α} x-ray and to reduce background counts. We succeeded in observing a scattering pattern of satellite peaks at 14.7 K in the AFP3 phase with accuracy high enough to estimate structure factors.

Figure 2 shows the x-ray diffraction patterns at 14.7 K (AFP3) after subtracting the background intensity measured at the paramagnetic region. Many satellite peaks indexed by the fundamental wave vector $\mathbf{k} = (0, 0, 2/7) [2\pi/c]$ and their higher harmonics were detected as in the previous x-ray study, except the peaks at $\xi = 2 \pm 4/7$ because of their small intensity. The satellite peak is composed of a main peak indicated by an arrow in Fig. 2 and a small side peak. These come from reflections of the $K_{\alpha 1}$ and $K_{\alpha 2}$ x ray, respectively. The Bragg reflections at the scattering vector of $\mathbf{Q} = \mathbf{G} = (0, 0, l)$ with $2 \leq l \leq 10$ were also measured in order to evaluate structure factors for the satellites, though the data are not shown here.

The integrated intensities of the satellites as well as the Bragg reflections were transformed to squared values of structure factors by corrections of Lorentz

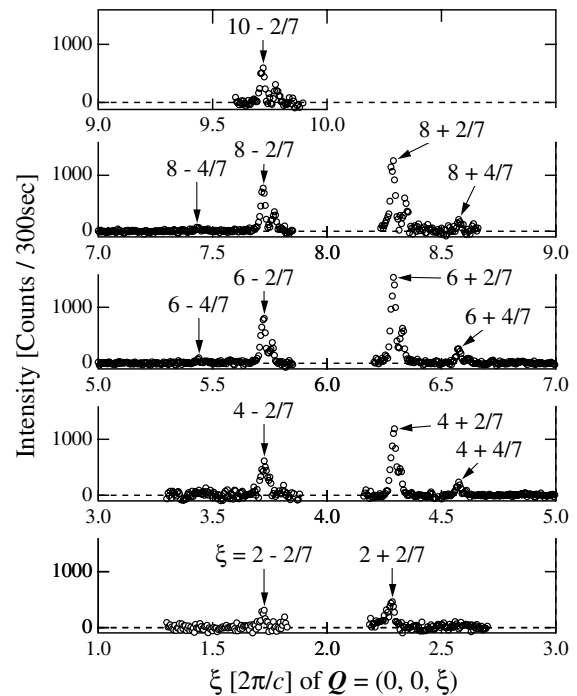


FIG. 2. X-ray diffraction patterns on the reciprocal-lattice line $[0, 0, \xi]$ of CeSb at 14.7 K in the AFP3 phase.

factor, polarization factor, absorption factor, extinction factor, and Debye-Waller factor. The details in these corrections will be presented elsewhere. For convenience to discuss the superlattice model afterward, we evaluated the ratios of the squared magnitudes of structure factors of the satellites to those for the fundamental Bragg reflections, $|F_S(\mathbf{Q})|^2 / |F_B(\mathbf{Q})|^2$. The results are represented by open circles in Fig. 3. It should be noted that, within each Brillouin zone, the magnitude of squared structure factor at $\mathbf{G} - \mathbf{k}$ is much smaller than that at $\mathbf{G} + \mathbf{k}$. Generally, any crystal-lattice modulation cannot produce such asymmetric structure factors at $\mathbf{G} \pm \mathbf{k}$, because modulation amplitudes of the components for $\pm \mathbf{k}$ are same. This fact will be discussed again later.

In order to analyze the observed satellite reflection pattern, structure factors for x-ray diffraction involving both crystal-lattice and $4f$ -electron-orbital-state modulations which correspond to the magnetic structure are calculated.

First, we define the crystal-lattice modulation as in the previous study [16]. The squared-up superlattice structure in the AFP3 phase is schematically shown in Fig. 4(a) with δ for a lattice-modulation parameter. The model with one parameter δ has already been found to be sufficient to reproduce the intensity ratios of the higher-harmonic satellites to the fundamental one, as shown in Ref. [16]. The distance between neighboring Ce-ion layers of Γ_7 state is defined as d . The distance between neighboring Γ_8 -like (Γ_{80}) Ce-ion layers is assumed to be shorter by a factor of δ , so that it is defined as $d(1 - \delta)$. Then, the distance between the layers of Γ_{80} and Γ_7 Ce states can be defined as $d(1 - \delta/2)$. The Sb ions are supposed to be displaced

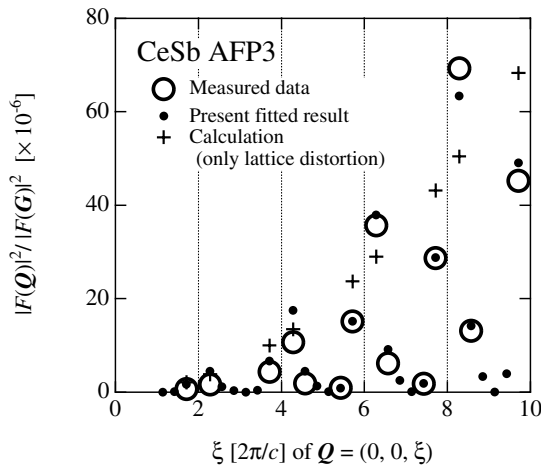


FIG. 3. Ratios of squared structure factors for the satellite peaks relative to those of the Bragg reflections. Open circles represent the experimental data. Solid circles are a fitted result based on the model of the modulations of a crystal lattice and a $4f$ -electron orbit. Crosses are a calculated result for the first harmonic satellites considering only the lattice modulation with $\delta = 0.0018$.

together with the neighboring Ce ions in the ferromagnetic $(0\ 0\ 1)$ plane, because of the p - f mixing between them.

Next, the contribution of the modulation of the $4f$ -electron state in CeSb to the structure factors is considered as follows. As mentioned above, in the magnetically ordered state, the layers of Ce ions with the $4f$ -electron orbital states of Γ_7 and Γ_{80} stack in a complex sequence as depicted in Fig. 4(a). These orbital states give different atomic form factors for Ce ions f_7 and f_{80} , respectively. The value of f_{80} along the $[0\ 0\ 1]$ direction is expected to be larger than f_7 , because the electronic distribution of the Γ_{80} state is anisotropically extending in the $[1\ 0\ 0]$ - $[0\ 1\ 0]$ plane, whereas that of the Γ_7 state is rather isotropic. We calculated these atomic form factors of Ce ions in CeSb based on the realistic $4f$ -electron wave functions. The pioneering work on atomic form factors of a spherical $4f$ -electron orbit was performed by Keating in the x-ray diffraction study of superlattices of Ho in the magnetically ordered phase [17]. The scattering amplitude is represented by a matrix element, $\langle \Psi | e^{i\mathbf{Q}\cdot\mathbf{r}} | \Psi \rangle$, where $|\Psi\rangle$ is a wave function of atomic state. Recently, in the study of noncollinear orbital structures coexisting with multiaxial magnetic structures in rare-earth compounds, the scattering amplitudes were calculated for various magnetic rare-earth ions based on the Stevens equivalent-operator method [18]. In the present study of CeSb, we adopted their method to evaluate the form factors of the $4f$ electron of Ce^{3+} ions. The Γ_7 and Γ_{80} states are expressed with basis functions $|J_z\rangle$ as

$$|\Gamma_7\rangle = \sqrt{\frac{5}{6}} \left| +\frac{3}{2} \right\rangle - \sqrt{\frac{1}{6}} \left| -\frac{5}{2} \right\rangle, \quad (1)$$

$$|\Gamma_{80}\rangle = \alpha \left| +\frac{5}{2} \right\rangle + \sqrt{1 - \alpha^2} \left| -\frac{3}{2} \right\rangle. \quad (2)$$

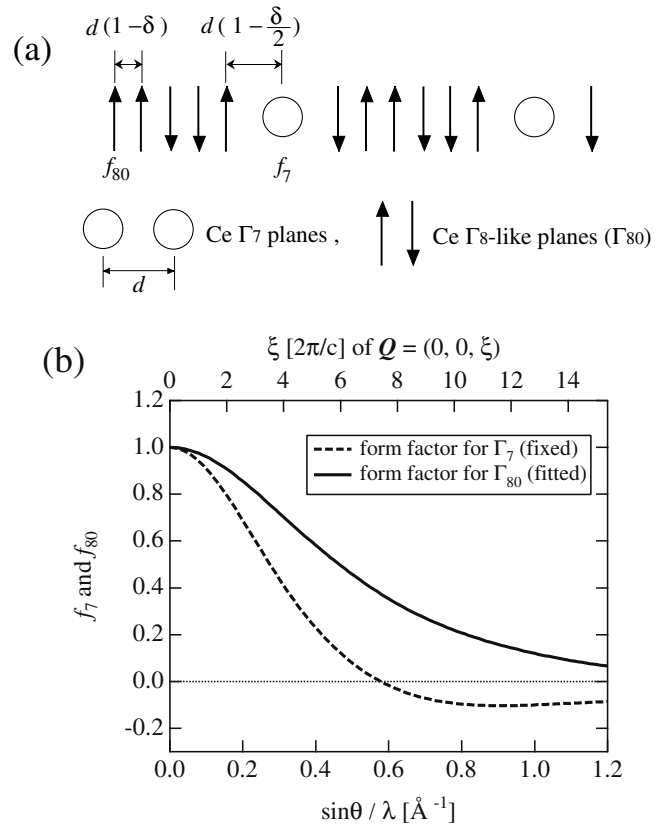


FIG. 4. (a) Schematic representation of the superlattice structure in the AFP3 phase with the indications of interlayer distances and atomic form factors in the model. (b) The $4f$ -electron atomic form factor f_{80} for the ordered Ce ions determined from the fitting procedure and f_7 calculated for the paramagnetic Γ_7 Ce-ion state.

For the pure Γ_8 state, α is equal to $\sqrt{5/6}$. Using Eqs. (1) and (2), we obtained the $4f$ -electron form factors f_7 and f_{80} . The rest form-factor component due to electrons except $4f$ is assumed to be the calculated one for a spherical Ce^{4+} ion. The form factor of Sb ions was also quoted from Ref. [19].

Then, the structure factor for the x-ray scattering from the system is calculated by using the simple formula as

$$F(\mathbf{Q}) = \sum_j f_j(\mathbf{Q}) e^{i\mathbf{Q}\cdot\mathbf{r}_j}. \quad (3)$$

Here $f_j(\mathbf{Q})$ is the atomic form factor of the j th atom. The atomic position \mathbf{r}_j in the modulated structure is expressed by the parameter δ . The modulation of the $4f$ -electron state is taken into account in the calculation by putting the form factors f_7 or f_{80} on the paramagnetic and ordered Ce-ion sites, respectively, in the layered structure as shown in Fig. 4.

We performed a least-squares fitting of the numerically calculated structure factors including the two kinds of modulation to the experimental data in the AFP3 phase with free parameters of α and δ . The result is shown in Fig. 3 by solid circles. The calculation reproduces the experimental data satisfactorily. The resultant parameters are

$\alpha = 1.00 \pm 0.06$ and $\delta = (1.80 \pm 0.02) \times 10^{-3}$. The value of δ is almost the same as that obtained in the previous study. The value of $\alpha = 1.00$ means that the ordered Ce ions possess the fully saturated magnetic state under the $J = 5/2$ multiplet of Ce ion, which is consistent with the neutron diffraction results of the magnetic structures [6]. The determined $4f$ -electron form factor f_{80} for the ordered Ce ions as well as the calculated f_7 are shown in Fig. 4(b). The difference between f_{80} and f_7 is less than 0.4 in the unit of electron number.

The asymmetric diffraction pattern around a fundamental Bragg reflection can be understood as the result of the interference effect between reflections due to lattice and charge-density modulations. In order to demonstrate the importance of the interference effect, $|F_S(\mathbf{Q})|^2/|F_B(\mathbf{Q})|^2$ of the first harmonics satellite peaks were calculated for the case of only the lattice modulation characterized by δ determined in the present analysis. It is apparent that the result shown in Fig. 3 by crosses does not coincide with the data. Thus, the modulation of the $4f$ -electron state, that is, the charge-density modulation, is the key issue to understand the observed x-ray superlattice diffraction pattern of CeSb. On the other hand, if we consider only the $4f$ -electron modulation by taking $\delta = 0$, the value of $|F_S(\mathbf{Q})|^2/|F_B(\mathbf{Q})|^2$ is around 2×10^{-6} . It is less than the observable limit by the present experimental accuracy. Therefore, the tiny difference of the form factors of Ce ions in the different $4f$ -electron orbital states becomes detectable due to the interference effect described above.

In conclusion, the present x-ray diffraction study gives direct evidence for the strong modulation of the $4f$ -electron orbital state as well as the crystal lattice modulation in the magnetically ordered state of CeSb. These modulations are associated with the coexistence of different $4f$ -electron states; the crystal field ground state Γ_7 and almost fully polarized Γ_8 -like state caused by the spatially enhanced p - f mixing effect. Recently, the same phenomenon was observed in the magnetically ordered phases of CeP under high pressures, which will be reported in a forthcoming paper. These results give further support for the magnetic polaron mechanism with a strong p - f mixing effect to explain the $4f$ -electron state in the low-carrier system CeX.

Professor Y. Noda and Mr. T. Shobu are acknowledged for their fruitful discussions. The present study is partially supported by Grant-in-Aids No. 09044097 from the Ministry of Education, Culture, Sports, Science and Technology of Japan, and No. 11694093 from Japan Society for Promotion of Science.

[1] J. M. Effantin, J. Rossat-Mignod, P. Burlet, H. Bartholin, S. Kunii, and T. Kasuya, *J. Magn. Magn. Mater.* **47&48**, 145 (1985); R. Shiina, H. Shiba, and P. Thalmeier, *J. Phys. Soc. Jpn.* **66**, 1741 (1997).

- [2] T. Matsumura, S. Nakamura, T. Goto, H. Amitsuka, K. Matsuhira, T. Sakakibara, and T. Suzuki, *J. Phys. Soc. Jpn.* **67**, 612 (1998); P. Link, A. Gukasov, J.-M. Mignot, T. Matsumura, and T. Suzuki, *Phys. Rev. Lett.* **80**, 4779 (1998).
- [3] Y. Murakami, J. P. Hill, D. Gibbs, M. Blume, I. Koyama, M. Tanaka, H. Kawata, T. Arima, Y. Tokura, K. Hirota, and Y. Endoh, *Phys. Rev. Lett.* **81**, 582 (1998).
- [4] K. Hirota, N. Oumi, T. Matsumura, H. Nakao, Y. Wakabayashi, Y. Murakami, and Y. Endoh, *Phys. Rev. Lett.* **84**, 2706 (2000); Y. Tanaka, T. Inami, T. Nakamura, H. Yamauchi, H. Onodera, K. Ohoyama, and Y. Yamaguchi, *J. Phys. Condens. Matter* **11**, L505 (1999).
- [5] See, for example, T. Suzuki, *Physical Properties of Actinide and Rare Earth Compounds*, JJAP Series 8 (Publication Office, Japanese Journal of Applied Physics, Tokyo, 1993), p. 267; *Physica (Amsterdam)* **186B-188B**, 347 (1993).
- [6] J. Rossat-Mignod, J. M. Effantin, P. Burlet, T. Chattopadhyay, L. P. Regnault, H. Bartholin, C. Vettier, O. Vogt, D. Ravot, and J. C. Achard, *J. Magn. Magn. Mater.* **52**, 111 (1985).
- [7] H. Heer, A. Furrer, W. Hälg, and O. Vogt, *J. Phys. C, Solid State Phys.* **12**, 5207 (1979).
- [8] H. Takahashi and T. Kasuya, *J. Phys. C* **18**, 2697 (1985); **18**, 2709 (1985); **18**, 2721 (1985); **18**, 2731 (1985); **18**, 2745 (1985); **18**, 2755 (1985); T. Kasuya and T. Suzuki, *J. Phys. Soc. Jpn.* **61**, 2628 (1992).
- [9] R. Siemann and B. R. Cooper, *Phys. Rev. Lett.* **44**, 1015 (1980); N. Kioussis, B. R. Cooper, and A. Banerjee, *Phys. Rev. B* **38**, 9132 (1988).
- [10] B. Hälg, A. Furrer, and O. Vogt, *Phys. Rev. Lett.* **54**, 1388 (1985); B. Hälg and A. Furrer, *Phys. Rev. B* **34**, 6258 (1986).
- [11] M. Kohgi, K. Iwasa, and T. Osakabe, *Physica (Amsterdam)* **281&282B**, 417 (2000).
- [12] M. Kohgi, T. Osakabe, K. Iwasa, J. M. Mignot, I. N. Goncharenko, P. Link, Y. Okayama, H. Takahashi, N. Mōri, Y. Haga, and T. Suzuki, *Rev. High Pressure Sci. Technol.* **7**, 221 (1998).
- [13] F. Hulliger, M. Landolt, H. R. Ott, and R. Schmelzler, *J. Low Temp. Phys.* **20**, 269 (1975).
- [14] M. Sera, T. Fujita, T. Suzuki, and T. Kasuya, *Valence Instabilities*, edited by P. Wachter and H. Boppert (North-Holland Publishing Company, Amsterdam, 1982), p. 435.
- [15] K. Iwasa, M. Kohgi, H. Ohsumi, K. Tajima, T. Takeuchi, Y. Haga, A. Uesawa, and T. Suzuki, *J. Phys. Soc. Jpn.* **68**, 881 (1999).
- [16] K. Iwasa, Y. Arakaki, M. Kohgi, and T. Suzuki, *J. Phys. Soc. Jpn.* **68**, 2498 (1999).
- [17] D. T. Keating, *Phys. Rev.* **178**, 732 (1969).
- [18] M. Amara and P. Morin, *J. Phys. Condens. Matter* **10**, 9875 (1998); M. Amara, R. M. Galéra, P. Morin, and J. F. Bérar, *J. Phys. Condens. Matter* **10**, L743 (1998).
- [19] E. N. Maslon, A. G. Fox, and M. A. O'Keefe, *International Tables for Crystallography Volume C*, edited by A. J. C. Wilson (Kluwer Academic Publishers, Dordrecht, 1992), p. 476.
- [20] T. Shobu, Y. Noda, A. Hannan, K. Iwasa, M. Kohgi, and T. Suzuki (to be published).